

Monitoring and assessment of seasonal land cover changes using remote sensing: a 30-year (1987–2016) case study of Hamoun Wetland, Iran

Rasoul Kharazmi · Ali Tavili ·
Mohammad Reza Rahdari · Lyudmila Chaban ·
Evgeny Panidi · Jesús Rodrigo-Comino

Received: 19 January 2018 / Accepted: 11 May 2018 / Published online: 23 May 2018
© Springer International Publishing AG, part of Springer Nature 2018

Abstract The availability of Landsat data allows improving the monitoring and assessment of large-scale areas with land cover changes in rapid developing regions. Thus, we pretend to show a combined methodology to assess land cover changes (LCCs) in the Hamoun Wetland region (Iran) over a period of 30-year (1987–2016) and to quantify seasonal and decadal landscape and land use variabilities. Using the pixel-based change detection (PBCD) and the post-classification comparison (PCC), four land cover classes were compared among spring, summer, and fall seasons. Our findings showed for the water class a higher correlation between spring and summer ($R^2 = 0.94$) than fall and spring ($R^2 = 0.58$) seasons. Before 2000, ~50% of the total

area was covered by bare soil and 40% by water. However, after 2000, more than 70% of wetland was transformed into bare soils. The results of the long-term monitoring period showed that fall season was the most representative time to show the inter-annual variability of LCCs monitoring and the least affected by seasonal-scale climatic variations. In the Hamoun Wetland region, land cover was highly controlled by changes in surface water, which in turn responded to both climatic and anthropogenic impacts. We were able to divide the water budget monitoring into three different ecological regimes: (1) a period of high water level, which sustained healthy extensive plant life, and approximately 40% of the total surface water was retained until the end of the hydrological year; (2) a period of drought during high evaporation rates was observed, and a mean wetland surface of about 85% was characterized by bare land; and (3) a recovery period in which water levels were overall rising, but they are not maintained from year to year. After a spring flood, in 2006 and 2013, grassland reached the highest extensions, covering till more than 20% of the region, and the dynamics of the ecosystem were affected by the differences in moisture. The Hamoun wetland region served as an important example and demonstration of the feedbacks between land cover and land uses, particularly as pertaining to water resources available to a rapidly expanding population.

R. Kharazmi · L. Chaban
Faculty of Applied Cosmonautics and Photogrammetry, Moscow State University of Geodesy and Cartography, Moscow, Russian Federation

A. Tavili · M. R. Rahdari (✉)
Faculty of Natural Resources, University of Tehran, Karaj, Iran
e-mail: Rahdarimr@gmail.com
e-mail: Rahdari@ut.ac.ir

E. Panidi
Department of Cartography and Geoinformatics, Saint Petersburg State University, Saint Petersburg, Russian Federation

J. Rodrigo-Comino
Instituto de Geomorfología y Suelos, Department of Geography, University of Málaga, Málaga, Spain

J. Rodrigo-Comino
Department of Physical Geography, Trier University, Trier, Germany

Keywords Multispectral imagery · Landsat · Landscape monitoring · Change detection · Image processing · Dry land · Wetland

Introduction

Land uses and land cover changes are one of the main driving forces of land degradation processes in the Earth system (Verburg et al. 2011). Understanding land use changes is indispensable to assess environmental changes (Amato et al. 2015; Chappell et al. 2018) and develop sustainable land plans (Bell et al. 2010; Debolini et al. 2015; Najafinasab et al. 2015; Li et al. 2017). Remote sensing can be defined as a tool that is able to assess these changes without physical contact. Remote sensing has been widely used because of its multidisciplinary applicability in geology (Siegal and Gillespie 1980; Immerzeel et al. 2014; Amri et al. 2017), forest evolution (Lim et al. 2003; Silva et al. 2017; Santos et al. 2017), natural hazard (Pourghasemi et al. 2012), hydrological processes (Schmugge et al. 2002; Etehadi Abari et al. 2017), geomorphology (Verstappen 1977; Moosavi et al. 2014; Kumar et al. 2018), vegetation vigor analysis (Jones and Vaughan 2010; Jabbari et al. 2015), land cover (Matinfar et al. 2013; Sabr et al. 2016), and land degradation (Zehtabian et al. 2014; Alanis et al. 2017; Ahmady-Birgani et al. 2017). Nowadays, remote sensing data are one of the most common resources to evaluate and monitor landscape evolutions and making reliable approaches for land cover changes (LCCs) (Schulz et al. 2010; Zewdie and Csaplovics 2015; Yuan et al. 2016; Kharazmi et al. 2016; Kharazmi et al. 2017b). Using multispectral imagery obtained from Landsat, it is possible to generate valuable data in non-well-studied regions (Shengbo and Rao 2008; Roy et al. 2014; Mandanici and Bitelli 2015).

The research of LCCs focuses on how surface landscapes evolve as a combination of different ecological terrains. Previous studies of LCCs have helped establish optimal distributions of human land uses (agricultural, urban, etc.) and aimed to protect the resources and stability of local populations (e.g., Luyssaert et al. 2014; Mirzaei et al. 2016; Sakieh and Salmannahiny 2016). Driving factors that contribute to LCCs include human activities (Fu 2003; Nazari Samani et al. 2016a), political and economic decisions around urbanization and infrastructure (Yli-Pelkonen 2008; Briner et al. 2012; Bateman et al. 2013), and environmental changes (Shajaat Ali 2006; Szczypta et al. 2015). Land cover can be considered as the natural interface between ecological and anthropogenic activities (Rahdari et al. 2013; Yuan et al. 2016), affecting at the local and global scales (Luo et al. 2008; Issanova et al. 2015; Nazari Samani et al. 2016c).

The population growth rate of arid regions is roughly three times higher than the world average (Goudie 2013). Under the combined effects of climate change and population growth, semi-arid and arid regions have undergone severe stresses on local resources (Baron et al. 1998; Ranjeet et al. 2009). Many of these regions are difficult to access, making studies of these areas particularly problematic. Fortunately, during the last decade, the abundance of available remotely sensed data has helped to expand LCC monitoring efforts (Lu and Weng 2007; Rashki et al. 2014; Xiao et al. 2017). In particular, Landsat images, with records as far back as 1972, enhance large-scale researches that also are able to incorporate temporal changes (Wulder et al. 2012; Roy et al. 2014). The high frequency of monitored time and the large coverage areas make Landsat images ideal for studying LCCs (Vogelmann et al. 2016; Dawelbait et al. 2017). Also, remote sensing provides valuable information about landforms (Nazari Samani et al. 2016b).

In arid territories, wetlands function as a part of the ecological landscape system (Mitsch and Gosselink 2000), which are essential because of their functions as a natural resource for million people (Dixon et al. 2016). Wetlands are characterized by a high water quality and are able to support high levels of biodiversity (Chen and Liu 2015). However, according to Patino and Estupinan-Suarez (2016), about half of the total worldwide wetland areas are being lost during the last century, causing a serious environmental problem for human and wildlife. The Ramsar Convention on wetlands in Iran (2014) reported that 24 international wetlands are located in Iran (1,486,438 ha) and some of them, due to human activities, have been highly polluted such as Anzali wetland (Vesali Naseh et al. 2012a; Vesali Naseh et al. 2012b; Hargalani et al. 2014), Hoor al-Azim wetland (Eydizadeh et al. 2014), and Hamoun wetland (Zolfaghari et al. 2016). Therefore, the protection of all of them should be vital for national and international organizations and policy makers. However, there is a lack of information about them since these drastic land degradation processes occurred. Previous studies of Iran's wetlands have mainly focused on environmental pollution aspects, but less attention has been paid to land cover changes. It would allow us developing land use plans to manage the potential degraded areas and performing models to anticipate possible irreparable environmental losses.

Therefore, the main aim of this study was to assess land cover changes using Landsat images for a non-well-studied wetland area (as the Hamoun wetland) located in southeastern Iran. The population of the Hamoun wetland area is characterized by rapid expansion, and continued monitoring and prediction of LCCs will be essential to evaluate their future socioeconomic needs. Thus, two specific goals must be achieved: (1) to determine when the most significant landscape changes should be expected on a seasonal time scale and (2) to determine which season has the least year-to-year variability during 30 years (1987–2016).

Materials and methods

Study area

The Hamoun wetland is located in the Sistan Basin in southeast Iran and is divided into three regions: Saberi, Puzak and Hirmand (Fig. 1a) (Najafi and Vatanfada 2011; Mousavi-Sabet et al. 2014; Maleki et al. 2016). The Hamoun Lake is the third largest lake of Iran, and in 2016, it was designated as a biosphere reserve by UNESCO. At its maximum extent, the Hamoun Lake averages 4 m water depth and is fed by the Hirmand

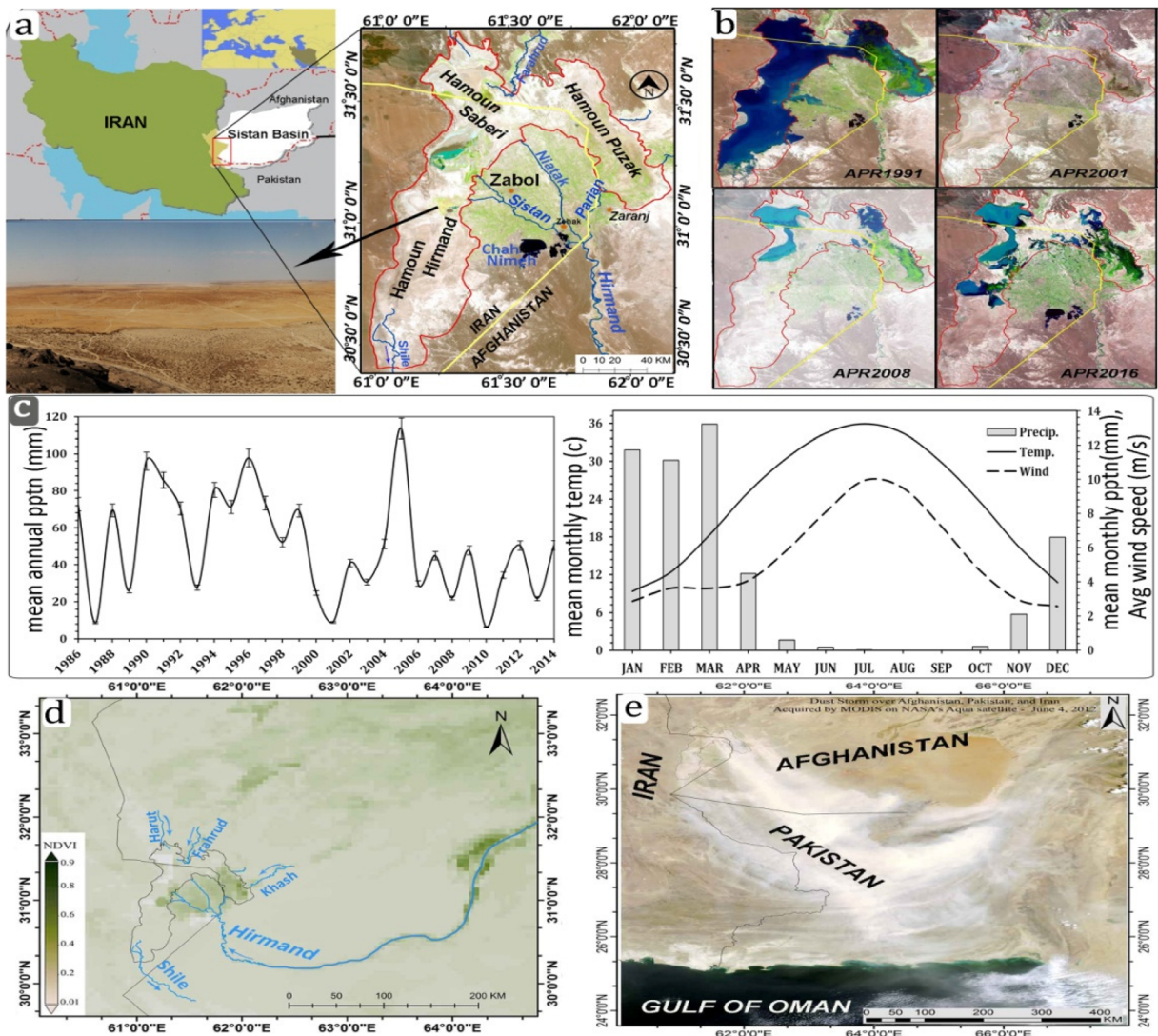


Fig. 1 a Study area. b Four springtime images showing the progressive drying and recovery of the Hamoun wetland. c Rain-fall and temperature variations during the studied period (Zabol

and Zahak synoptic climatic stations). d NDVI image of Sistan Basin (2016). e Distribution and sources of dusts for the Hamoun wetland (June 2012)

Table 1 Mean annual meteorological conditions of the study area

Station	Location	Precipitation (mm)	Temp (°C)	Wind (m/s)	Distance from case study (km)
Zabol*	31° 02' N, 61° 29' E	54	24.7	5.9	10
Zehak [†]	30° 54' N, 61° 41' E	45	22.3	5	20

*For the study period 1986–2014
[†]For the study period 1992–2014

River which supports local agriculture and a growing population (Yousefi et al. 2017). Low precipitation amounts and a high evaporation have driven this area into multiyear droughts during the last 30 years (Table 1, Fig. 1b–d). This region is characterized by 120-day winds (Rezazadeh et al. 2013; Ekhtesasi and Gohari 2013; Alizadeh-Choobari et al. 2014; Rezaei and Ghofranfarid 2018), which blow from the north from June to September (Rashki et al. 2013), making the Sistan Basin one of the windiest regions over the world (Fig. 1e). During periods of high water level, these winds are able to lead to an increase of air humidity, and during periods of low water level, to the deposition of dust (Kaskaoutis et al. 2015), both of which stress the environment and the local population. Recent studies of the Sistan Basin have focused on these dusts (Alizadeh-

Choobari et al. 2014; Behrooz et al. 2017), but further studies are very limited by the remoteness of the area.

Landsat image selection

Landsat images of the Hamoun wetland taken from 1987 to 2016, freely available online from the USGS (<https://earthexplorer.usgs.gov>), were surveyed to quantify distributions and changes of land cover types (Fig. 2). Landsat images have 30 m/pixel resolution and are taken every 16 days (Pekel et al. 2016). For each of the 30 years studied, two clear and noise-free images were selected for each season and the best available images in each season were selected (Table 2). By convention, spring was defined from March to May, summer from June to August, and the fall season from

Fig. 2 Flowchart of the methodology used for this research

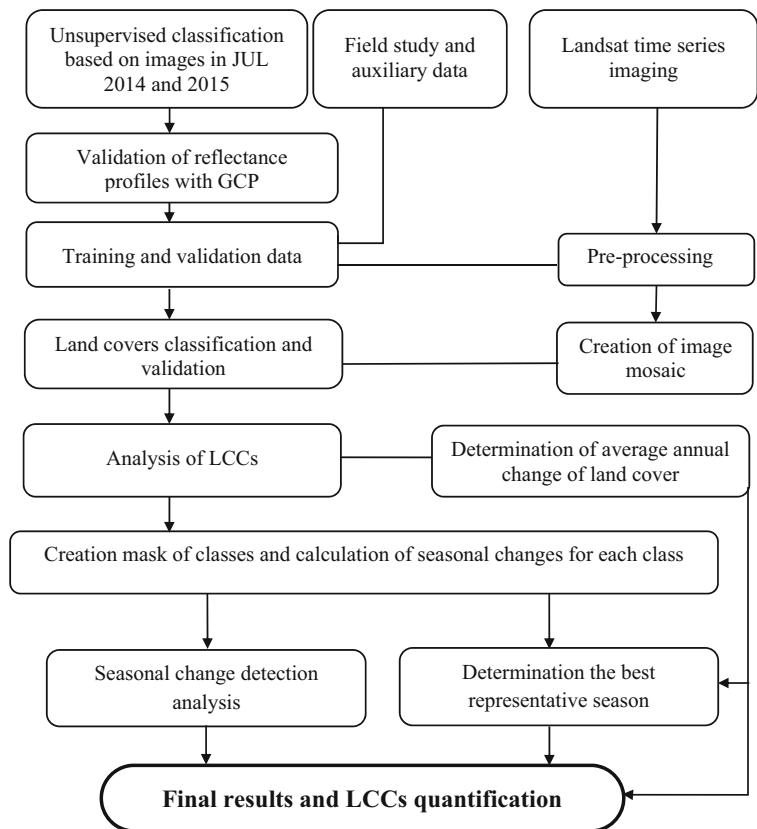


Table 2 Landsat images used in different seasons during the 30-year period (row 157, paths 38 and 39)

Sensor	Year	Spring	Summer	Fall
TM	1987	03 Mar	06 Jul	24 Sep
TM	1988	–	22 Jun	–
TM	1989	24 Mar	01 Jun	13 Sep
TM	1990	25 Apr	–	05 Dec
TM	1991	30 Mar	18 Aug	06 Nov
TM	1992	14 Apr	19 Jul	24 Nov
TM	1993	03 Mar	20 Jun	24 Sep
TM	1994	–	25 Jul	27 Sep
TM	1995	–	–	01 Nov
TM	1996	27 Mar	30 Jul	16 Sep
TM	1998	15 Apr	18 Jun	24 Oct
TM and ETM ⁺	1999	–	16 Jul (TM)	27 Oct (ETM ⁺)
TM	2000	04 Apr	25 Jul	11 Sep
ETM ⁺	2001	30 Mar	10 Jun	06 Sep
ETM ⁺	2002	18 Apr	08 Aug	11 Oct
ETM ⁺	2003	21 Apr	26 Jul*	14 Oct*
ETM ⁺ *	2004	07 Apr	10 Jun	16 Oct
ETM ⁺ *	2005	10 Apr	13 Jun	17 Sep
ETM ⁺ *	2006	29 Apr	16 Jun	06 Oct
ETM ⁺ *	2007	16 Apr	05 Jul	25 Oct
TM	2008	26 Apr	15 Jul	19 Oct
TM	2009	15 Mar	02 Jul	06 Oct
TM	2010	18 Mar	19 Jul	26 Nov
TM and ETM ⁺ *	2011	03 Apr (TM)	01 Aug (ETM ⁺)	04 Oct (ETM ⁺)
ETM ⁺ *	2012	29 Apr	19 Aug	06 Oct
OLI	2013	24 Apr	13 Jul	01 Oct
OLI	2014	27 Apr	30 Jun	18 Sep
OLI	2015	30 Apr	19 Jul	07 Oct
OLI	2016	18 Mar	21 Jul	23 Sep

*Operational despite scan line corrector (SLC) failure

September to November. Two images were necessary to ensure total coverage of the study area in each season. In winter season, due to the cloudy weather, assessments and interpretation of images could not be used. Thus, it was no possible to show significant changes in land cover from fall season to winter.

Moreover, for some years, Landsat data were not available, and after May 2003, a fault in the instrument caused a 22% loss of coverage in Landsat ETM⁺ images (Howard and Lacasse 2004; El Fellah et al. 2017). Fortunately, this defect affected <10% of the Hamoun study area and, for these gaps, land cover type was interpolated from the nearest neighbor pixels. In total, 154 Landsat images were processed for this research.

Landsat image treatments

An atmospheric correction and a conversion of the brightness values from radiance to reflectance (Vahtmäe and Kutser 2013; Feyisa et al. 2014; Bernardo et al. 2017) were performed using FLAASH (Fast Line-of-sight Atmospheric Analysis of Spectral Hypercubes) module in ENVI v. 5.1 (Othman et al. 2018). Atmospheric correction is not strictly necessary for image interpretation (Wu 2004), but the results obtained by Okin and Gu (2015) and El Fellah et al. (2017) showed that these algorithms allow improving the datasets.

The boundary of the study area encloses a total area of 5.95×10^5 ha, which supposes the total extension of the Hamoun Lake at its highest water level. That interpretation

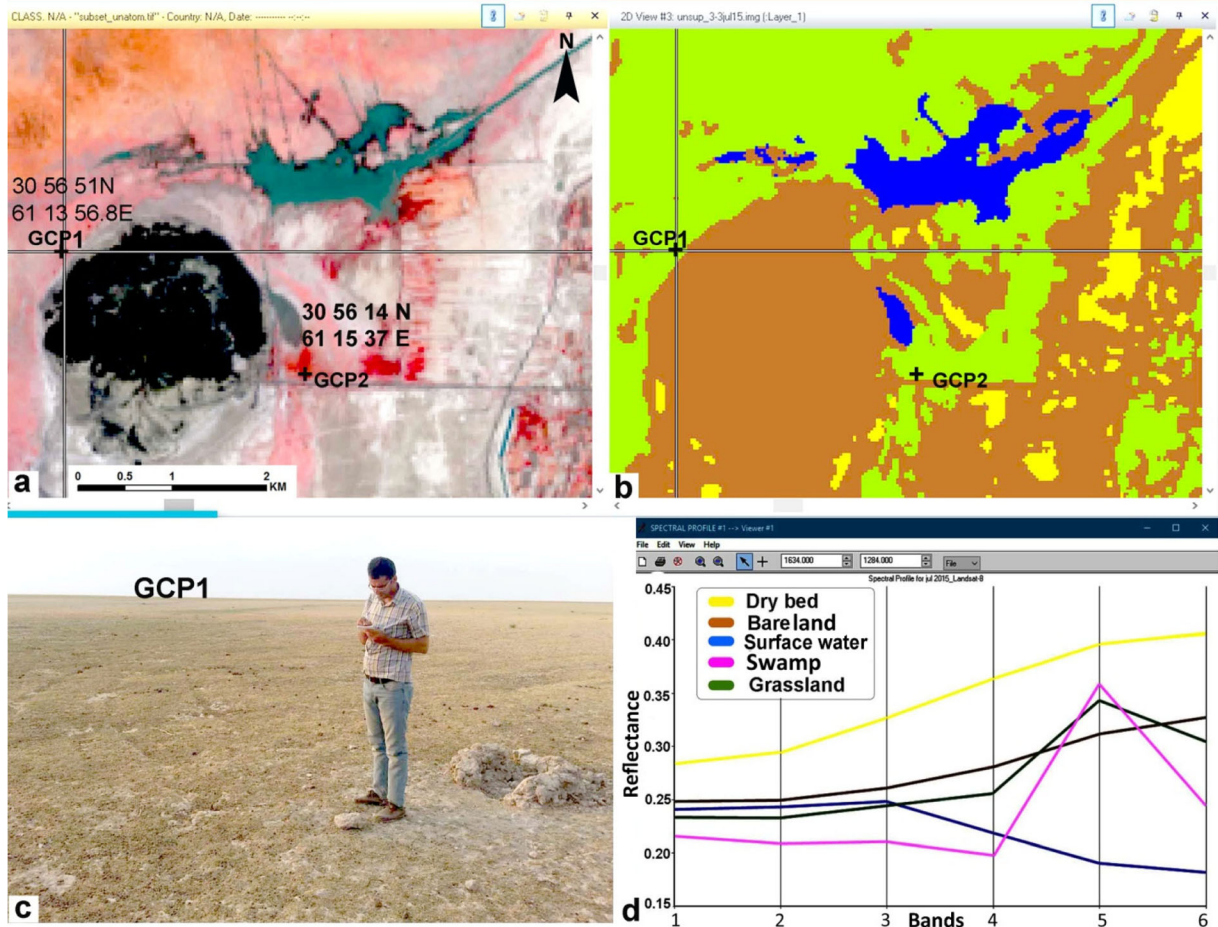


Fig. 3 Verification of model results. **a** Landsat images of a representative part of the studied area (July 2015). **b** Unsupervised land cover classification of **a** (the location of the ground control points (GCPs) in **a**, **b** is marked with a cross). **c** Example of representative

grassland area close to ground control point 1 (GCP1). **d** Reflectance profiles of the five types of land cover originally defined by the algorithm

can be noted from Google Earth images in Fig. 1a. Classification of the land cover was performed using the ERDAS Imagine maximum likelihood algorithm (Abd El-Kawy et al. 2011; Jaleta et al. 2016; Kharazmi et al.

2017b). According to Bolstad and Lillesand (1991), Gevana et al. (2015), and Rebelo et al. (2017), that approach, tying a training algorithm to ground-truth control data, is the most statistically robust in assessing remotely sensed images. In countries such as Iran where a limited ground control data occurs, this algorithm is ideal for that application. Unsupervised classification was conducted on two images from 30 June 2014 and 19 July 2015. Based on reflectance profiles, the region was mapped into five major classes of land cover: (1) surface water, (2) bare land, (3) dry bed, (4) swamp, and (5) grasslands. Then, 60 control points were randomly selected within the mapped area and were compared with the ground-truth observations. Those comparisons confirmed that the algorithm predicted the land cover type to within acceptable levels of accuracy (Fig. 3). The highest error was in

Table 3 Land cover classification types

Classification	Description
Surface water	Surface water bodies; in this case, the Hamoun Lake
Bare land	Areas devoid of vegetation, including salt flats
Swamp	Vegetated areas dominated by water-loving plant types (e.g., reeds)
Grasslands	Areas dominated by grass and low shrubs commonly used for livestock pasturing

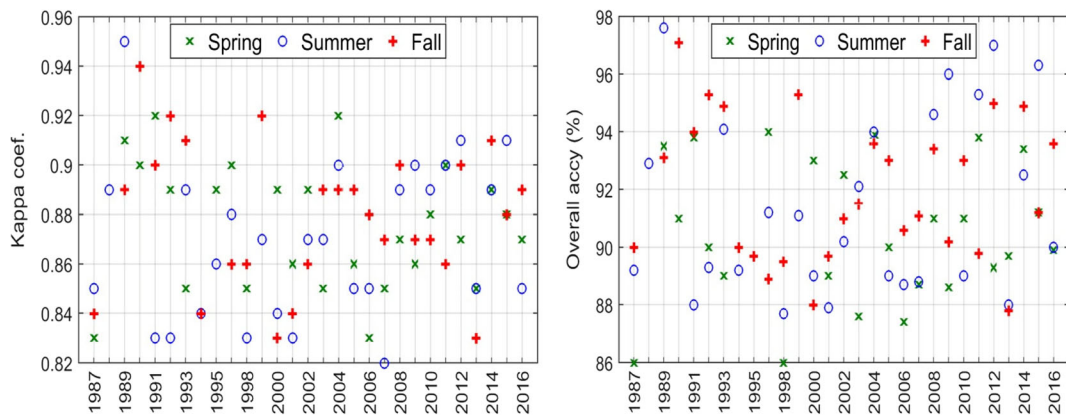


Fig. 4 Overall accuracy and kappa coefficient for classification of land cover types per season

distinguishing “bare land” and “dry bed” regions. Both of them were merged and named “bare land” to be referred to areas devoid of vegetation and surface water. The ERDAS algorithm was trained to identify land cover types using a combination of reflectance profiles, visual interpolation (Dawelbait et al. 2017), and Google Earth images

(Karkon Varnosfaderani et al. 2017) and to map the study area into water, swamp, grassland regions, and bare lands (Table 3).

To quantify LCCs, the pixel-based change detection (PBCD) was used for determining “from-to” changes in data that has already been classified into zones (post-

Table 4 Overall accuracy (%) and kappa coefficient in other arid and semi-arid regions

Study location	Overall accuracy	Kappa	Reference
Northwestern Ethiopia	89.9	0.87	Zewdie and Csaplovics (2015)
Western Nile Delta of Egypt	96	0.9	Abd El-Kawy et al. (2011)
Chile	70.2	0.75	Schulz et al. (2010)
Kenya	88	0.85	Kiage et al. (2007)
Northeast China	85	0.75	Shengbo and Rao (2008)
Australia	93.5	0.84	Rachael et al. (2011)
Egypt	93.8	0.91	Abdulaziz et al. (2009)
Nigeria	91.5	0.88	Kafi et al. (2014)
Sudan	89.2	0.81	Biro et al. (2013)
Turkmenistan	88.2	0.88	Maman et al. (2011)
Southeastern Australia	83.7	0.79	Gangjun (1996)
China	83.8	0.81	Ruan et al. (2008)
Faiyum Oasis, Egypt	95	0.91	Mandanici and Bitelli (2015)
Western Australia	85	0.8	Amiraslani and Dragovich (2013)
Khorasan, East Iran	84	0.67	Rezaei Moghaddam and Saghafi (2006)
South Egypt	96.7	0.95	Faid and Abdulaziz (2012)
Egypt	97.2	0.9	Bakr et al. (2010)
Northeastern Egypt	95	0.92	Badreldin and Goossens (2014)
South Central United States	88.2	0.75	Qin et al. (2016)
Northeastern Iraq	83.4	0.81	Al-Saady et al. (2015)
South Iraq	81.6	0.76	Jabbar and Zhou (2013)
Saudi Arabia	98.1	0.85	Rahman (2016)

Table 5 Correlation coefficient (R^2) of land types among each paired season

Land cover types	Spring-summer	Summer-fall	Fall-spring
Surface water	0.97	0.95	0.76
Swamp	0.63	0.64	0.52
Grasslands	0.20	0.60	0.40
Bare land	0.94	0.95	0.76

classification comparison) (Chen et al. 2012; Zewdie and Csaplovics 2015; Kharazmi et al. 2016; Demissie et al. 2017). Gain was defined as the percentage of a land cover class that is added from t_1 to t_2 and loss as the percentage of elimination of that land cover. Land cover classes that did not change among times were called persistent. Additionally, swap was calculated to account for shifts in the land cover where the percentage cover was conserved. Swap is the simultaneous loss and gain of area for a given land cover type, but in different regions within the study area. For a land use class (m), the amount of swap (S_m) was calculated as

$$S_m = 2 \times \min (a_m - b_m, c_m - b_m)$$

where a_m is the total column proportion of the land cover class, b_m represents the pixel persistence of the land cover class (Padonou et al. 2017), and c_m means the total row proportion of the land cover class. Additionally, the total change of a land cover type was either the sum of the net change and the swap or the sum of the gains and losses.

Results and discussion

The accuracy of the mapping procedure was calculated by ERDAS Imagine based on the field study results of 2014 and 2015 (see above), visual interpretation using a

standard RGB composite display of some images in the time series (e.g., Karkon Varnosfaderani et al. 2017; Dawelbait et al. 2017), Google Earth images, and recent literature on this area. Based on Yuan et al. (2016), the reliability of estimates of LCCs can be approximated by the image classification accuracy. The overall accuracy of our classification was between 81.3 and 97.6%, and the kappa index (Foody 2002) was between 0.83 and 0.94 (Fig. 4). An overall accuracy of 70% or more (Chuang et al. 2011) was considered a successful classification and mapping of the study area (Table 4).

Over the 30 years of the research period, the surface water area was highly predictable from spring to summer ($R^2 = 0.94$) and from summer to fall ($R^2 = 0.91$) (Tables 5, 6, and 7). From summer to fall, surface water extent decreased, causing a corresponding increase in the extent of grasslands ($R^2 = 0.36$) and bare land ($R^2 = 0.90$).

Annual summertime changes in vegetation, dependent on spring humidity, resulted in a low correlation in the extent of grassland between fall and spring ($R^2 = 0.18$) (Fig. 5). Bare land was highly predictable from summer to fall ($R^2 = 0.90$), showing a slight decrease going into the later season. Bare land was the lowest during spring and the highest during the fall, relating to the counter-balancing changes in surface water and grasslands (Fig. 5).

From 1988 to 1998, surface water dominated the study area, comprising more area than any other land category for all seasons in most of this decade (Fig. 6). During this period, the Hamoun Lake reached at its peak and the results of this study demonstrated its subsequent decline. From 2000 to 2004, the Hamoun Lake became nearly completely dry, constituting the lowest water level of the lake during the 30-year study period (Fig. 6). Correspondingly, the extent of bare land, including dry exposed lakebed, increased dramatically during this period. The expansion of bare land accelerated after 2000, and during two periods (2000–2004 and 2011–2016),

Table 6 Standard regression analysis (F value)

Land cover types	Spring-summer		Summer-fall		Fall-spring	
	F	Sig	F	Sig	F	Sig
Surface water	345.88	0.00	158.4	0.00	11.8	0.003
Swamp	11.16	0.004	5.234	0.014	7.58	0.012
Grasslands	1.10	0.304	12.40	0.002	4.49	0.047
Bare land	152.4	0.000	213.1	0.000	28.0	0.000

Table 7 Standard regression analysis (*T* value)

Land cover types	Spring-summer				Summer-fall				Fall-spring			
	Constant		Spring		Constant		Summer		Constant		Fall	
	<i>T</i>	Sig	<i>T</i>	Sig	<i>T</i>	Sig	<i>T</i>	Sig	<i>T</i>	Sig	<i>T</i>	Sig
Surface water	-3.456	0.002	18.5	0.000	-1.51	0.149	12.5	0.000	2.87	0.111	3.44	0.003
Swamp	-0.278	0.784	3.34	0.004	0.158	0.877	2.86	0.014	4.08	0.001	2.75	0.012
Grasslands	4.18	0.000	1.05	0.304	0.68	0.500	3.52	0.002	2.60	0.017	2.12	0.047
Bare land	0.146	0.885	12.3	0.000	6.88	0.000	14.5	0.000	-0.823	0.420	5.2	0.000

the bare land class covered more than 90% of the region, reaching maximum values of 99% in 2004 (Figs. 6 and 11). On a seasonal scale, the greatest extent of bare land was in fall (Fig. 6c).

Variations between the north and the southern areas included higher springtime water levels in the north (Saber, Puzak) relative to the south after 2000, and higher relative water levels in the south from 1991 to 1993 (Figs. 7, 8, and 9). This variation suggests that spring floods from the Farahood and Harut rivers have long been an important control on the water supply of region. After 2004, pulses of river discharge into the Hamoun Lake led to an increase in water level that was not maintained from year to year. Grassland was the most extensive in 2006 and 2013 during the spring, covering 22 and 23% of the total area of region, respectively. The 85% loss in grassland shortly after these periods is attributed to human intervention (e.g., overgrazing of livestock, Fig. 10). Repeated water discharge into the Hamoun wetland was recorded from 2005 to 2010 (Figs. 6, 7, 8, and 9), although during summer, an increase in temperatures and dry periods avoided water level increases.

In 2005 after a significant flood, grassland experienced the most gain (23%) and, then during the subsequent years, a lost higher than 80% of its total extension (Fig. 12). From 2007 to 2011, spring floods were additionally correlated with an increase in grassland extension, although grassland cover is typically the dominant ecological control of dry land ecosystems (e.g., Dubovyk et al. 2016; Gessner et al. 2013). Our findings demonstrated that very little fluctuation occurred in total grassland areas in comparison to variations in swamp and surface water land types.

To smooth short-time-scale variations in LCCs caused by seasonal changes, Fig. 6d shows the annual

average values for each land cover type. Furthermore, the swamp and surface water land types were combined to highlight changes in the presence and absence of vegetation relative to water-logged landscapes (Fig. 11). Our results showed that the grasslands exhibited a very little fluctuation relative to the highly fluctuating one conformed by the water swamp class in the Hamoun wetland area, but in other wetlands, vegetation cover is entitled as a main factor for LCCs (Munyati 2000; Tareq et al. 2004; Sosnowski et al. 2016). We considered that grasslands were not the best indicators for analyzing dynamics of Hamoun wetland, because no significant changes were observed during a long-term period (Fig. 6d). The combined water class (watery land with vegetation) showed a general decreasing trend that is expected to continue, with high fluctuations into the coming decade. LCCs occurred at different rates during the 30 years covered in this study, and changes in water level had the most significant effect on the health of this ecosystem. Many studies based on periodic long-term monitoring, carried out in the Hamoun wetland (Vekerdy et al. 2006; Shafie et al. 2011; Sharifikia 2013; Rashki et al. 2013; Kharazmi et al. 2017a; Maleki et al. 2018), are not comparable with our study because they do not allow obtaining an objective forecast of the real ecological situation. Our results showed that long-term monitoring assessments based on seasonal changes can provide more logical and precise results of ecosystem dynamics too.

The fall season was least affected by highly variable controls on the water level (e.g., spring flooding or summer heat waves) and was determined by this study to be the best representative season for continued long-term studies of the Hamoun wetland. Data from the fall season were the most representative of the annual means, and therefore, monitoring of this season can be

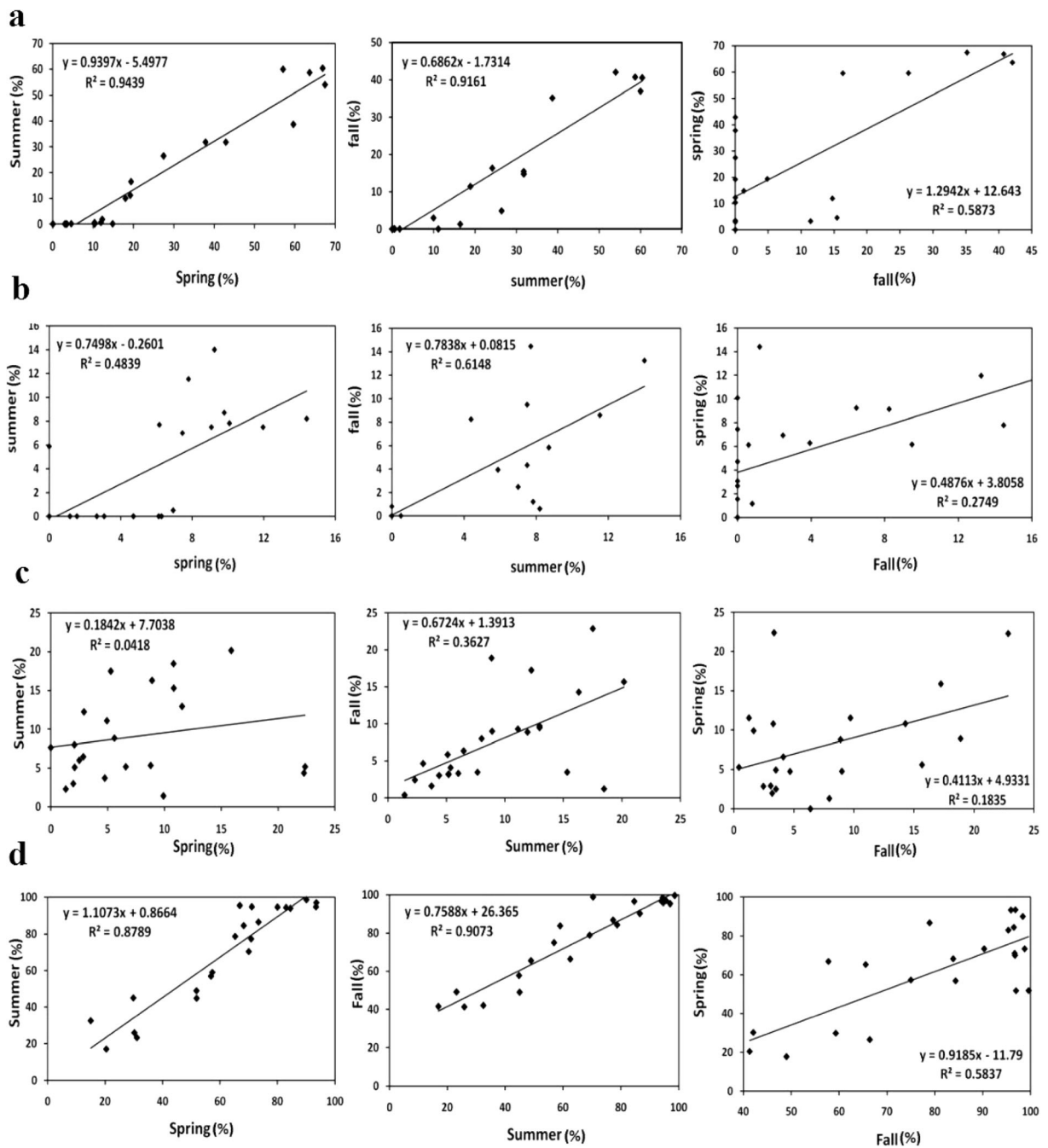


Fig. 5 Land cover comparisons among seasons. **a** Surface water. **b** Swamp. **c** Grasslands. **d** Bare land

considered as the most effective proxy of inter-annual variability (as it was seen in snapshots of time). The increasing trend in the extent of bare land could be the result of a positive feedback between overgrazing, exposed bare land, wind erosion, and plant-choking dust deposition in semi-arid and arid lands as confirmed by

several authors (Pulido-Fernández et al. 2013; Zezin et al. 2015; Borrelli et al. 2016). In this way, several authors also claimed that bare lands enhance land degradation processes related to soil erosion (Berendse et al. 2015; Ahmed et al. 2016), loss of biodiversity, and impoverishment of nutrients (Borrelli et al. 2014;

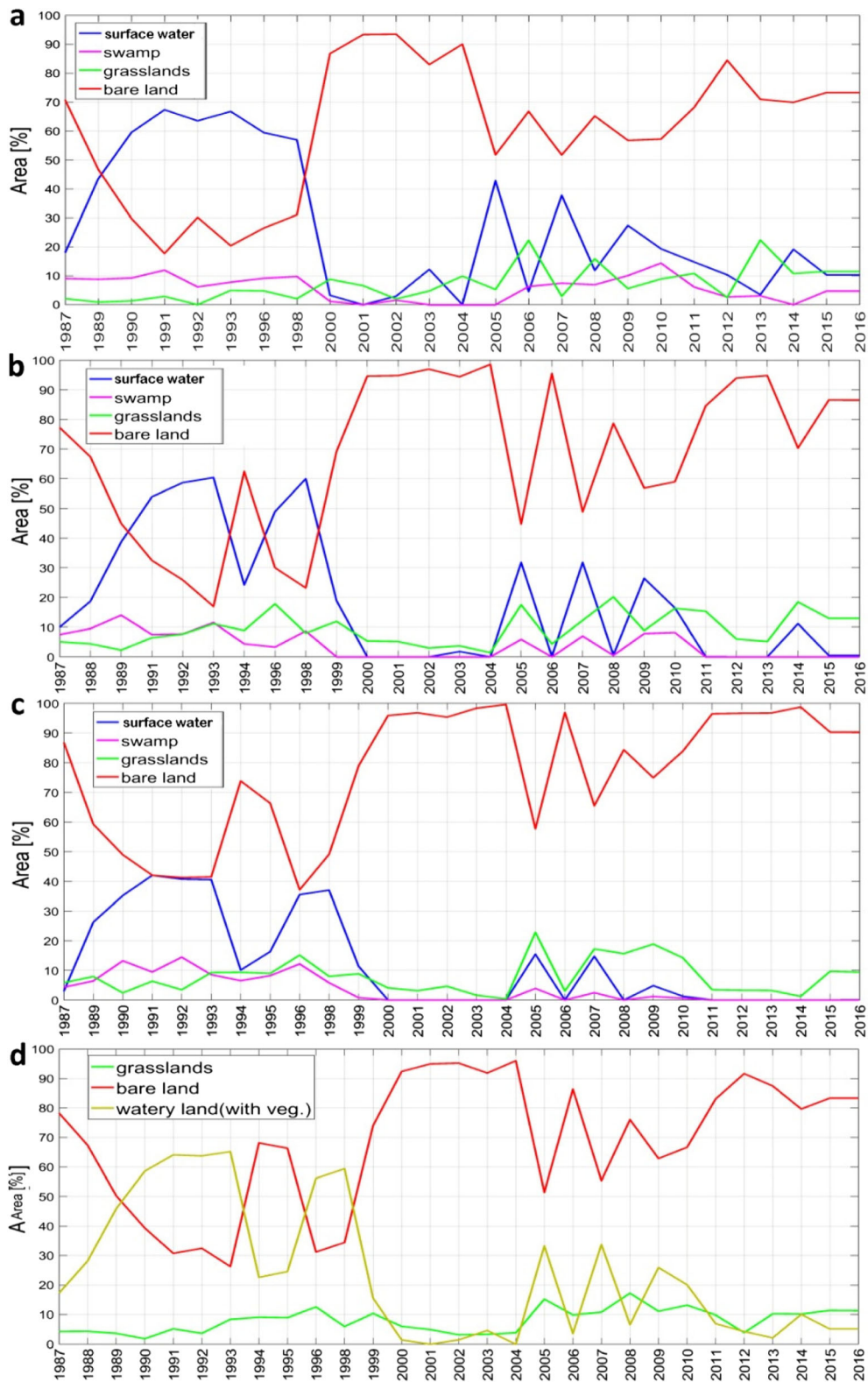


Fig. 6 Distributions of land cover types from 1987 to 2016. **a** Spring. **b** Summer. **c** Fall. **d** Mean annual land cover with a single combined class for swamp and surface water classes

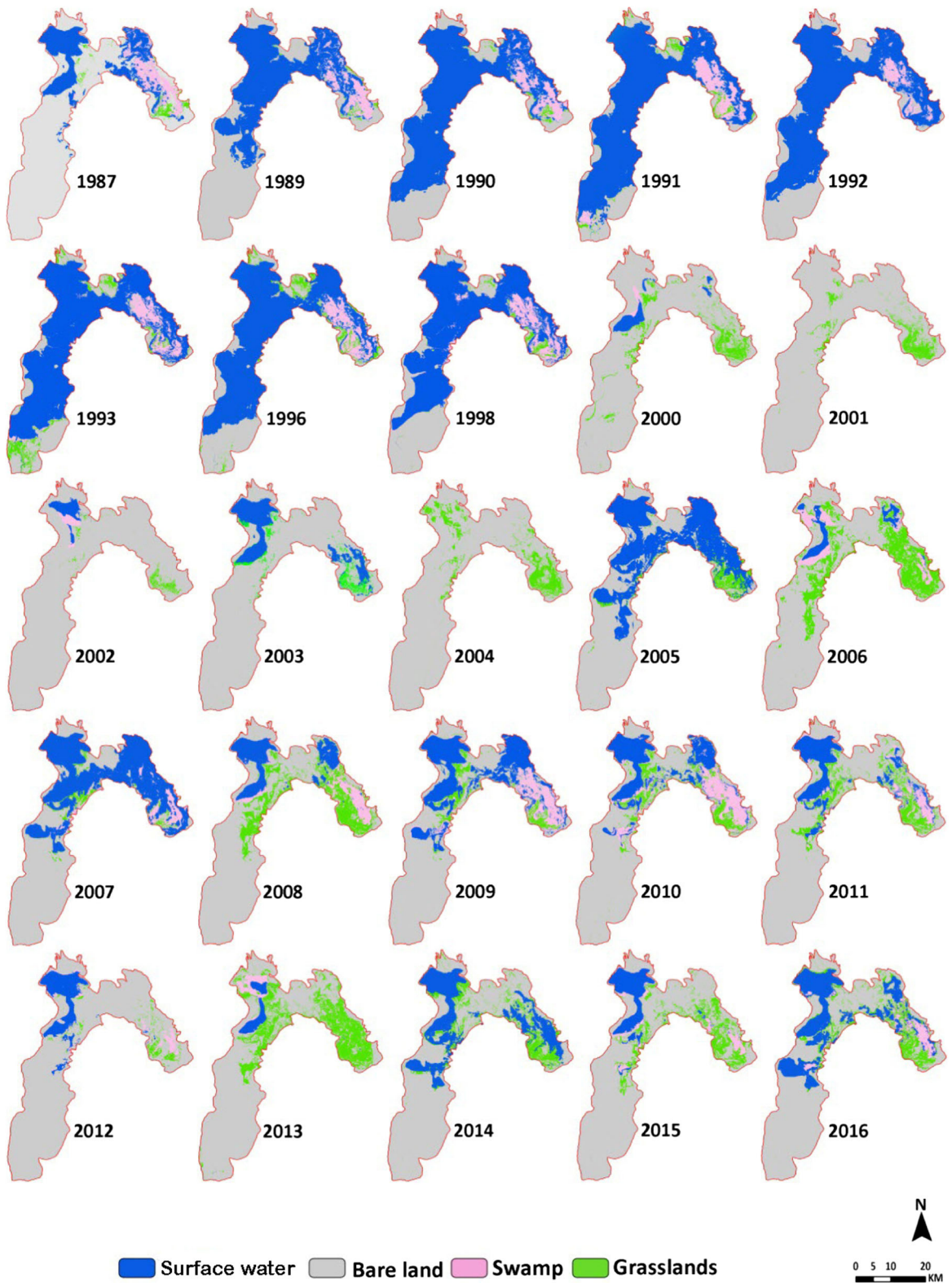


Fig. 7 Land cover changes in the study area during spring

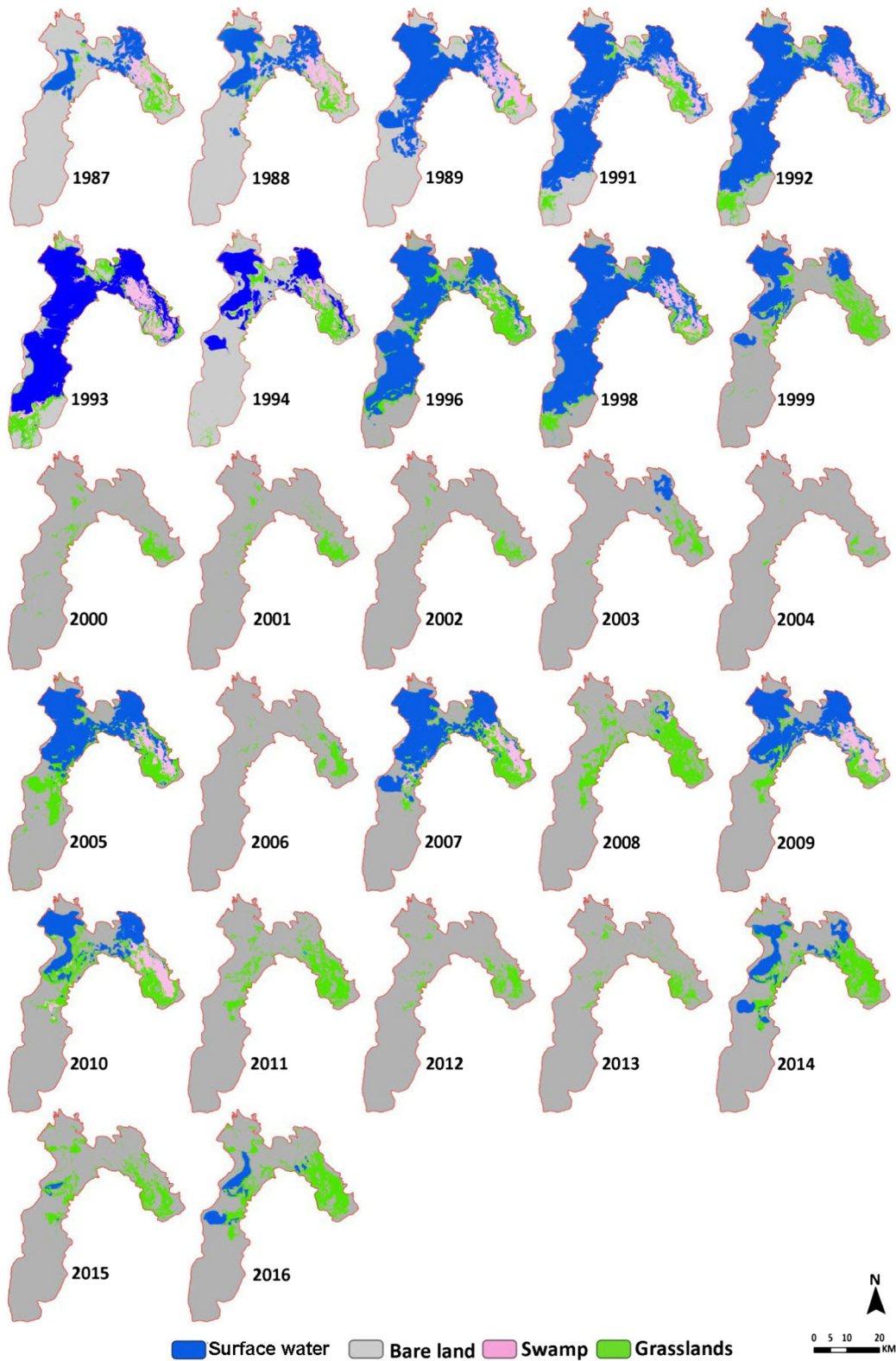


Fig. 8 Land cover changes in the study area during summer

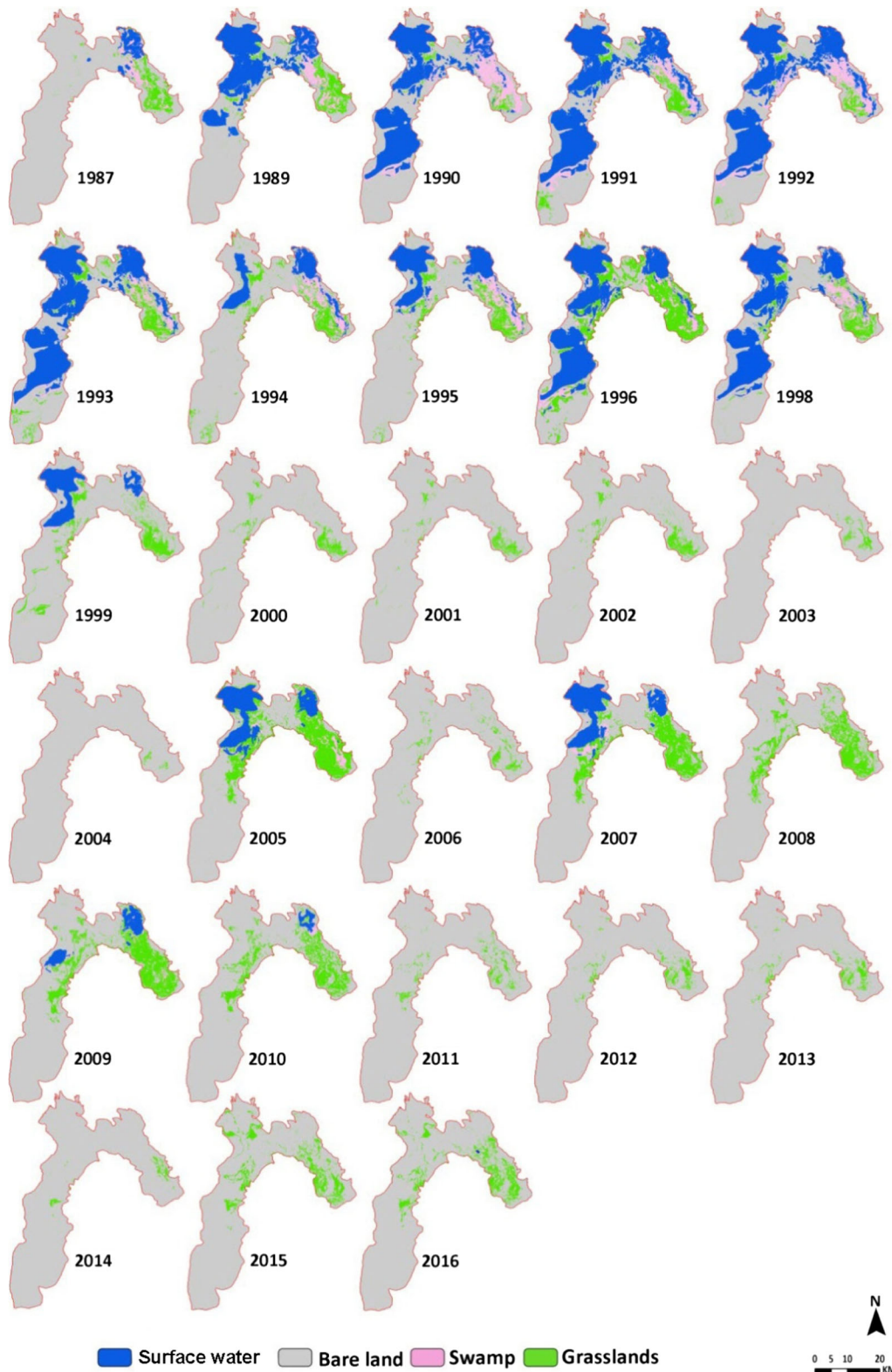


Fig. 9 Land cover changes in the study area during fall



Fig. 10 Examples of grassland in the Hamoun wetland. Black arrows indicate anthropogenic activities associated with nomads livestock over grazing

Nearing et al. 2017). According to that, policy makers and rural populations have to develop effective solutions such as revegetation strategies and the use of amendments, geotextiles, or mulches (Bienes et al. 2016; Hueso-Gonzalez et al. 2016). Naturally, these strategies have to be conducted in order to take into account the mentioned driving factors such as water competence, long dry periods, and land use changes such as grazing or abandonment (Lasanta et al. 2000; Lasanta et al. 2015).

Using the fall season as a representative proxy of the inter-annual variability, the highest gains (26%) in watery land (with vegetation) occurred in 1989 and 1995. Conversely, the most significant losses occurred in 1999 when the extent of surface water dropped by 31% (Fig. 12). Despite this variability, the persistence values of the water land class showed that water as a resource was available from 1987 to 1999, which demonstrated

that ecosystem dynamics were healthier during this period. After 2000, water levels were extremely lower and then showed fluctuations unable to recover to the levels of the previous decade. The water land class exhibited high levels of swap in 1989 (20% of the class value). Additionally, grassland swap was high in 1999 (10% of the class value). Significant changes in water lands and grasslands show both net change and total change from 2005 to 2008 (Fig. 12).

More than 25% of the total jobs in this region involve the care of livestock which pasture in the Hamoun area (Dahmardeh et al. 2009). Therefore, over half of the inhabitants of the Sistan Basin will be directly affected by changes to the Hamoun wetland. We confirmed that the desertification process is leading to a decrease in vegetation cover, particularly annual vegetation and grassland on which the livestock feed. In Fig. 10, it can be observed how grazing resources were limited to

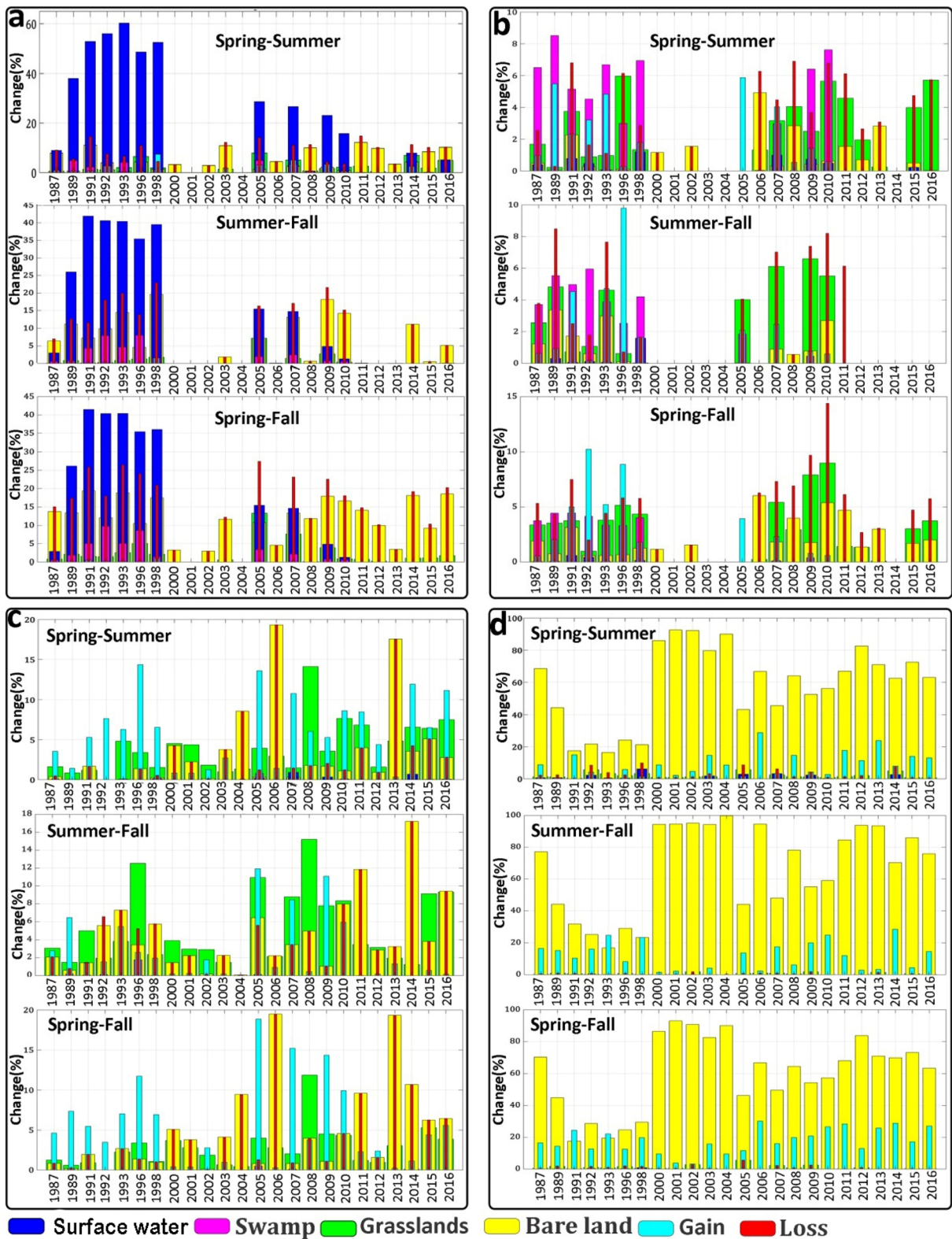


Fig. 11 Inter-annual LCCs during different seasons. a Surface water. b Swamp class. c Grasslands class. d Bare land

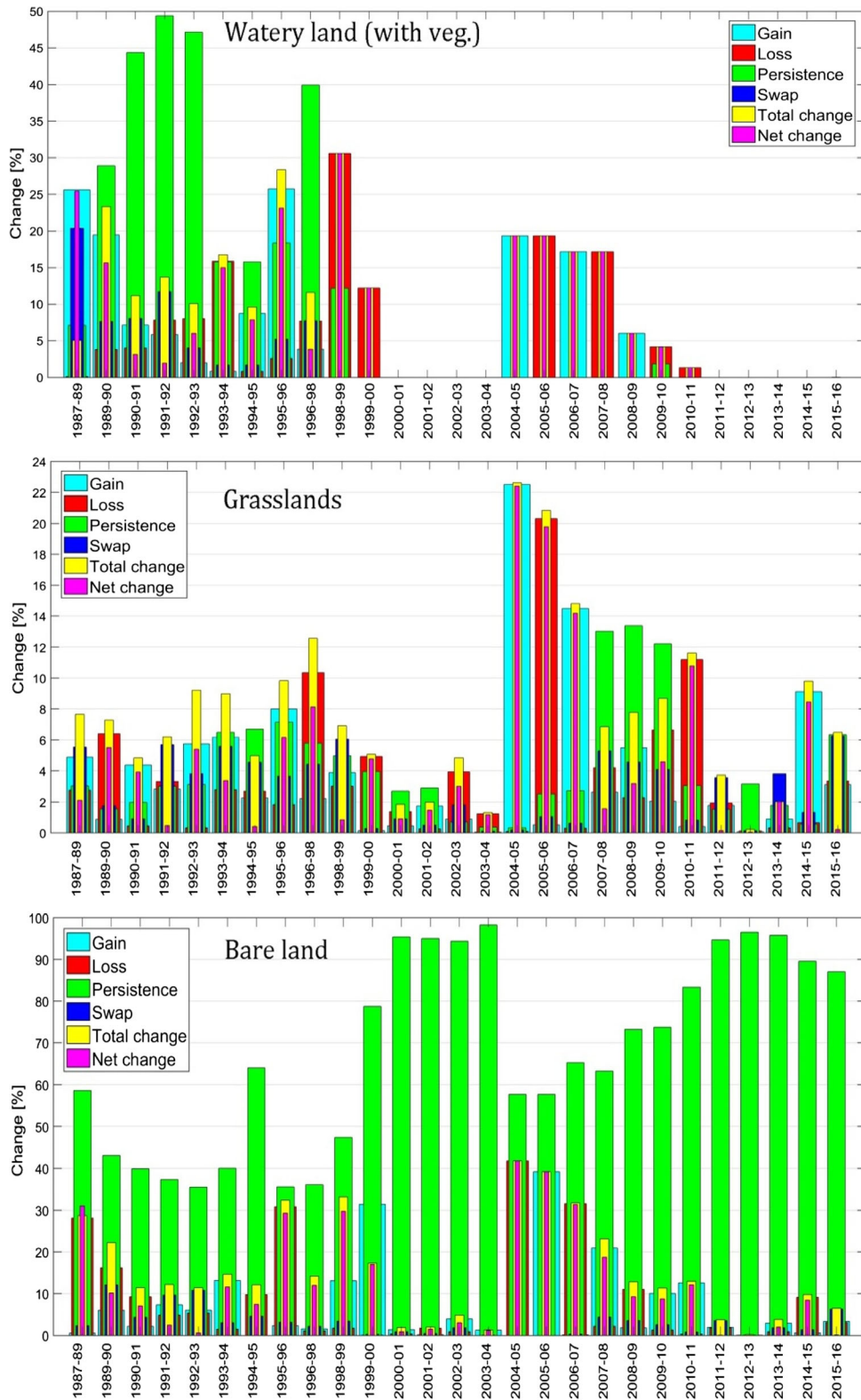


Fig. 12 Annual LCCs from 1987 to 2016

small areas of the wetland, where enough moisture existed to sustain grasslands. Overgrazing in these limited areas exposed wetlands to wind erosion (Kairis et al. 2015) and led to the spread of drought-tolerant plants and invasive species in rapidly dewatering regions (Flory and D'Antonio 2015).

Furthermore, changes in land cover distribution showed three distinct periods in the recent history of the Hamoun wetland, each of which can be attributed to a change in the available water budget (Figs. 6d, 7, 8, and 9). Firstly, a wet system period (1988–1998) is in its prime, balancing ~40% surface water with vegetation and comparable bare land exposures. Fed continually by plentiful rivers, the Hamoun wetland maintained a significant amount of water over this decade, sustaining the small population with a steady water supply. Secondly, a dry system period (1999–2004) is when Hamoun wetland experienced a significant drought which included the almost complete desiccation of the lake and the absence of sustained swamplands. The evaporation increased, and the water supply from upstream watersheds decreased, being likely a result of harsher climatic conditions during this time. This period represents the most severe hydrologic conditions in the Hamoun wetland. Finally, thirdly, a recovering system period (2005–2016) is when spring floods from the rivers are feeding the Hamoun Lake episodically, increasing the water level. However, during the summertime, climatic conditions instigated high evaporation rates again and these levels were not maintained from year to year. An associated increase in vegetation areas showed a sustaining influence on the fluctuating water level, suggesting that the system is in recovery from the drought period, but it is not yet able to reestablish the wet system by its self.

Causes of the drought are hypothesized to be a variety or combination of factors including a lack of water supply into the lake, increasing population, increasing agricultural and grazing areas, a decrease of water storage in the four main reservoirs (“Chah Nimeh” holding 1530 Mm³ of water; Vekerdy et al. 2006), and a new construction of two dams in Afghanistan (“Kajaki” and “Kmal Khan”; Whitney 2006). Therefore, we claim that this study of LCCs demonstrates the fragility of the Hamoun wetland ecosystem and the unstable feedbacks among winds,

dust mobilization, and high evaporation rates that stressed and drove the ecological system to its current recovering state.

Conclusions

Characterizing landscape changes and evolutions in the Hamoun wetland demonstrated the importance of the application solutions for local water budgets, and the necessity to quantify these dynamics and impacts on the ecosystem at the local and regional scales. We observed that the Hamoun wetland showed several fluctuations over short-time scales and that its seasonal variability at long-term trends can provide insights into the future evolution of the landscape. Water loss over the last 30 years has pushed the region from a period of fertility and ecological health to a period of drought and desertification and, finally, to a recovering ecological regime. This recovering state reflects both the expansion of the grassland in response to an increase of water input and the instability of that grassland for overgrazing. This study further determined that (1) fall was the best season for long-term monitoring, being the most representative of the inter-annual variability; (2) water levels were the highest during spring, a result attributed to springtime flooding and fall-winter precipitation; (3) conversely, water levels were the lowest in fall after high evaporation rates during hot and dry summer seasons; (4) vegetation, in both swamp and grassland terrains, showed the lowest expansion from 2000 to 2005 when the drought stressed and reduced the extent of water-loving plant life; and (5) wet-environment land classes (surface water and swamp) exhibited the most inter-annual variability, and the responses of grassland extent to that change in water supply were universally less extreme. We conclude that this study case provides further evidence of ecological transformation in the Middle East and desertification processes associated with both global warming and anthropogenic landscape forcing.

Acknowledgments We would like to show our gratitude to Dr. Mackenzie Day at the University of Washington, USA, for having valuable comments and sharing her pearls of wisdom with us about proofreading the manuscript during this research. Finally, we also express our sincere gratitude to the Editor-in-Chief and Managing Editor of the *Environmental Monitoring and Assessment* journal as well as to the two anonymous reviewers for their insights.

References

- Abd El-Kawy, O. R., Rod, J. K., Ismail, H. A., & Suliman, A. S. (2011). Land use and land cover change detection in the Western Nile Delta of Egypt using remote sensing data. *Applied Geography, 31*(2), 483–494.
- Abdulaziz, A. M., José, M., Hurtado, J., & Al Douri, R. (2009). Application of multitemporal Landsat data to monitor land cover changes in the Eastern Nile Delta region, Egypt. *International Journal of Remote Sensing, 30*(11), 2977–2996.
- Ahmady-Birgani, H., McQueen, K. G., Moeinaddini, M., & Naseri, H. (2017). Sand dune encroachment and desertification processes of the Rigboland Sand Sea, Central Iran. *Scientific Reports, 7*(1), 1523.
- Ahmed, M., Al-Dousari, N., & Al-Dousari, A. (2016). The role of dominant perennial native plant species in controlling the mobile sand encroachment and fallen dust problem in Kuwait. *Arabian Journal of Geosciences, 9*(2), 134.
- Alanis, N., Hernández-Madriral, V. M., Cerda, A., Muñoz-Rojas, M., Zavala, L. M., & Jordan, A. (2017). Spatial gradients of intensity and persistence of soil water repellency under different forest types in Central Mexico. *Land Degradation & Development, 28*(1), 317–327.
- Alizadeh-Choobari, O., Zavar-Reza, P., & Sturman, A. (2014). The “wind of 120 days” and dust storm activity over the Sistan Basin. *Atmospheric Research, 143*, 328–341.
- Al-Saady, Y., Merkel, B., Al-Tawash, B., & Al-Suhail, Q. (2015). Land use and land cover (LULC) mapping and change detection in the Little Zab River Basin (LZRB), Kurdistan region, NE Iraq and NW Iran. *FOG - Freiberg Online Geoscience, 43*, 1–32.
- Amato, F., Havel, J., Gad, A. A., & El-Zeiny, A. M. (2015). Remotely sensed soil data analysis using artificial neural networks: a case study of El-Fayoum depression, Egypt. *ISPRS International Journal of Geographical Information, 4*(2), 677–696.
- Amiraslani, F., & Dragovich, D. (2013). Image acquisition for detection of vegetation change based on long-term rainfall in an arid rangeland in Western NSW, Australia. *Environmental Earth Sciences, 70*(1), 83–95.
- Amri, K., Rabai, G., Benbakhti, I. M., & Khennouche, M. N. (2017). Mapping geology in Djelfa District (Saharan Atlas, Algeria), using Landsat 7 ETM+ data: an alternative method to discern lithology and structural elements. *Arabian Journal of Geosciences, 10*(4), 87.
- Badreldin, N., & Goossens, R. (2014). Monitoring land use/land cover change using multi-temporal Landsat satellite images in an arid environment: a case study of El-Arish, Egypt. *Arabian Journal of Geoscience, 7*(5), 1671–1681.
- Bakr, N., Weindorf, D. C., Bahnassy, M. H., Marei, S. M., & El-Badawi, M. M. (2010). Monitoring land cover changes in a newly reclaimed area of Egypt using multi-temporal Landsat data. *Applied Geography, 30*(4), 592–605.
- Baron, J. S., Hartman, M. D., Kittel, T. G. F., Band, L. E., Ojima, D. S., & Lammers, R. B. (1998). Effects of land cover, water redistribution, and temperature on ecosystem processes in the south Platte basin. *Ecological Applications, 8*(4), 1037–1051.
- Bateman, I. J., Harwood, A. R., Mace, G. M., Watson, R. T., Abson, D. J., Andrews, B., Binner, A., Crowe, A., Day, B. H., Dugdale, S., Fezzi, C., Foden, J., Hadley, D., Haines-Young, R., Hulme, M., Kontoleon, A., Lovett, A. A., Munday, P., Pascual, U., Paterson, J., Perino, G., Sen, A., Siriwardena, G., van Soest, D., & Termansen, M. (2013). Bringing ecosystem services into economic decision-making: land use in the United Kingdom. *Science, 341*(6141), 45–50.
- Behrooz, R. D., Esmaili-Sari, A., Bahramifar, N., & Kaskaoutis, D. (2017). Analysis of the TSP, PM10 concentrations and water-soluble ionic species in airborne samples over Sistan, Iran during the summer dusty period. *Atmospheric Pollution Research, 8*(3), 403–417.
- Bell, S., Alves, S., De Oliveira, E. S., & Zuin, A. (2010). Migration and land use change in Europe: a review. *Living Reviews in Landscape Research, 4*, 1–49.
- Berendse, F., van Ruijven, J., Jongejans, E., & Keesstra, S. (2015). Loss of plant species diversity reduces soil erosion resistance. *Ecosystems, 18*(5), 881–888.
- Bernardo, N., Watanabe, F., Rodrigues, T., & Alcântara, E. (2017). Atmospheric correction issues for retrieving total suspended matter concentrations in inland waters using OLI/Landsat-8 image. *Advances in Space Research, 59*(9), 2335–2348.
- Bienes, R., Marques, M. J., Sastre, B., Garcia-Diaz, A., & Ruiz-Colmenero, M. (2016). Eleven years after shrub revegetation in semiarid eroded soils. Influence in soil properties. *Geoderma, 273*, 106–114.
- Biro, K., Pradhan, B., Buchroithner, M., & Makeschin, F. (2013). Land use/land cover change analysis and its impact on soil properties in the northern part of Gadarif region, Sudan. *Land Degradation and Development, 24*(1), 90–102.
- Bolstad, P. V., & Lillesand, T. (1991). Rapid maximum likelihood classification. *Photogrammetric Engineering and Remote Sensing, 57*(1), 67–74.
- Borrelli, P., Ballabio, C., Panagos, P., & Montanarella, L. (2014). Wind erosion susceptibility of European soils. *Geoderma, 232*, 471–478.
- Borrelli, P., Panagos, P., Ballabio, C., Lugato, E., Weynants, M., & Montanarella, L. (2016). Towards a Pan European assessment of land susceptibility to wind erosion. *Land Degradation & Development, 27*(4), 1093–1105.
- Briner, S., Elkin, C., Huber, R., & Grêt-Regamey, A. (2012). Assessing the impacts of economic and climate changes on land-use in mountain regions: a spatial dynamic modeling approach. *Agriculture, Ecosystems & Environment, 149*, 50–63.
- Chappell, A., Webb, N. P., Guerschman, J. P., Thomas, D. T., Mata, G., Handcock, R. N., Leys, J. F., & Butler, H. J. (2018). Improving ground cover monitoring for wind erosion assessment using MODIS BRDF parameters. *Remote Sensing of Environment, 204*, 756–768.
- Chen, M., & Liu, J. (2015). Historical trends of wetland areas in the agriculture and pasture interlaced zone: a case study of the Huangqihai Lake Basin in Northern China. *Ecological Modelling, 318*, 168–176.
- Chen, X., Chen, J., Shi, Y., & Yamaguchi, Y. (2012). An automated approach for updating land cover maps based on integrated change detection and classification methods. *ISPRS Journal of Photogrammetry and Remote Sensing, 71*, 86–95.
- Chuang, C.-W., Lin, C.-Y., Chien, C.-H., & Chou, W.-C. (2011). Application of Markov-chain model for vegetation

- restoration assessment at landslide areas caused by a catastrophic earthquake in Central Taiwan. *Ecological Modelling*, 222(3), 835–845.
- Dahmardeh, M., Dahmardeh, M., Yazdani, S., & Piri, E. (2009). The socio-economic effects of Hamoon Lake in Sistan region of Iran. *Journal of Food, Agriculture and Environment*, 7(2), 799–802.
- Dawelbait, M., Dal Ferro, N., & Morari, F. (2017). Using Landsat images and spectral mixture analysis to assess drivers of 21-year LULC changes in Sudan. *Land Degradation & Development*, 28(1), 116–127.
- Debolini, M., Schoorl, J. M., Temme, A., Galli, M., & Bonari, E. (2015). Changes in agricultural land use affecting future soil redistribution patterns: a case study in southern Tuscany (Italy). *Land Degradation & Development*, 26(6), 574–586.
- Demissie, F., Yeshitila, K., Kindu, M., & Schneider, T. (2017). Land use/land cover changes and their causes in Libokemkem District of South Gonder, Ethiopia. *Remote Sensing Applications: Society and Environment*, 8, 224–230.
- Dixon, M. J. R., Loh, J., Davidson, N. C., Beltrame, C., Freeman, R., & Walpole, M. (2016). Tracking global change in ecosystem area: the wetland extent trends index. *Biological Conservation*, 193, 27–35.
- Dubovyk, O., Landmann, T., Dietz, A., & Menz, G. (2016). Quantifying the impacts of environmental factors on vegetation dynamics over climatic and management gradients of Central Asia. *Remote Sensing*, 8(7), 600.
- Ekhtesasi, M., & Gohari, Z. (2013). Determining area affected by dust storms in different wind speeds, using satellite images. *Desert*, 17(2), 193–202.
- El Fellah, S., Rziza, M., & El Haziti, M. (2017). An efficient approach for filling gaps in Landsat 7 satellite images. *IEEE Geoscience and Remote Sensing Letters*, 14(1), 62–66.
- Etehadi Abari, M., Majnounian, B., Malekian, A., & Jourgholami, M. (2017). Effects of forest harvesting on runoff and sediment characteristics in the Hyrcanian forests, northern Iran. *European Journal of Forest Research*, 136(2), 375–386.
- Eydizadeh, A., Eskandary, G. R., & Hashemi, S. A. R. (2014). Some biological aspect of *Carasobarbus luteus* (Heckel, 1843) in Hoor Al-azim wetland. *Scientific Journal of Biological Sciences*, 3(3), 29–36.
- Faid, A. M., & Abdulaziz, A. M. (2012). Monitoring land use change associated land development using multitemporal Landsat data and geoinformatics in Kom Ombo area, South Egypt. *International Journal of Remote Sensing*, 33(22), 7024–7046.
- Feyisa, G. L., Meilby, H., Fensholt, R., & Proud, S. R. (2014). Automated water extraction index: a new technique for surface water mapping using Landsat imagery. *Remote Sensing of Environment*, 140, 23–35.
- Flory, S. L., & D'Antonio, C. M. (2015). Taking the long view on the ecological effects of plant invasions. *American Journal of Botany*, 102(6), 817–818.
- Foody, G. M. (2002). Status of land cover classification accuracy assessment. *Remote Sensing of Environment*, 80(1), 185–201.
- Fu, C. (2003). Potential impacts of human-induced land cover change on East Asia monsoon. *Global and Planetary Change*, 37(3–4), 219–229.
- Gangjun, L. (1996). Land cover mapping in a salinised dryland farming area in southeastern Australia using Landsat TM data. *Geocarto International*, 11(4), 47–59.
- Gessner, U., Naeimi, V., Klein, I., Kuenzer, C., Klein, D., & Dech, S. (2013). The relationship between precipitation anomalies and satellite-derived vegetation activity in Central Asia. *Global and Planetary Change*, 110, Part A, 74–87.
- Gevana, D., Camacho, L., Carandang, A., Camacho, S., & Im, S. (2015). Land use characterization and change detection of a small mangrove area in Banacon Island, Bohol, Philippines using a maximum likelihood classification method. *Forest Science and Technology*, 11(4), 197–205.
- Goudie, A.S. (2013). Arid and semi-arid geomorphology. Cambridge University Press.
- Hargalani, F. Z., Karbassi, A., Monavari, S. M., & Abroomand Azar, P. (2014). A novel pollution index based on the bio-availability of elements: a study on Anzali wetland bed sediments. *Environmental Monitoring and Assessment*, 186(4), 2329–2348.
- Howard, S. M., & Lacasse, J. M. (2004). An evaluation of gap-filled Landsat SLC-off imagery for wildland fire burn severity mapping. *Photogrammetric Engineering and Remote Sensing*, 70(8), 877–880.
- Hueso-Gonzalez, P., Martínez-Murillo, J. F., & Ruiz-Sinoga, J. D. (2016). Effects of topsoil treatments on afforestation in a dry Mediterranean climate (southern Spain). *Solid Earth*, 7(5), 1479–1489.
- Immerzeel, W. W., Kraaijenbrink, P. D. A., Shea, J. M., Shrestha, A. B., Pellicciotti, F., Bierkens, M. F. P., & De Jong, S. M. (2014). High-resolution monitoring of Himalayan glacier dynamics using unmanned aerial vehicles. *Remote Sensing of Environment*, 150, 93–103.
- Issanova, G., Abuduwaili, J., Galayeva, O., Semenov, O., & Bazarbayeva, T. (2015). Aeolian transportation of sand and dust in the Aral Sea region. *International Journal of Environmental Science and Technology*, 12(10), 3213–3224.
- Jabbar, M. T., & Zhou, J. (2013). Environmental degradation assessment in arid areas: a case study from Basra Province, southern Iraq. *Environmental Earth Sciences*, 70(5), 2203–2214.
- Jabbari, S., Khajedin, S. J., Jafari, R., & Soltani, S. (2015). Remote sensing technology for mapping and monitoring vegetation cover (case study: Semirom-Isfahan, Iran). *Pollution*, 1(2), 165–174.
- Jaleta, D., Mbilinyi, B., Mahoo, H., & Lemenih, M. (2016). Evaluation of land use/land cover changes and Eucalyptus expansion in Meja watershed, Ethiopia. *Journal of Geography, Environment and Earth Science International*, 7(3), 1–12.
- Jones, H.G., Vaughan, R.A. (2010). Remote sensing of vegetation: principles, techniques, and applications. Oxford University Press.
- Kafi, K. M., Shafri, H. Z. M., & Shariff, A. B. M. (2014). An analysis of LULC change detection using remotely sensed data; a case study of Bauchi City. *IOP Conference Series: Earth and Environmental Science*, 20, 012056.
- Kairis, O., Karavitis, C., Salvati, L., Kounalaki, A., & Kosmas, K. (2015). Exploring the impact of overgrazing on soil erosion and land degradation in a dry Mediterranean agro-forest landscape (Crete, Greece). *Arid Land Research and Management*, 29(3), 360–374.

- Karkon Varnosfaderani, M., Kharazmi, R., Nazari Samani, A., Rahdari, M. R., Matinkhah, S. H., & Aslinezhad, N. (2017). Distribution changes of woody plants in western Iran as monitored by remote sensing and geographical information system: a case study of Zagros forest. *Journal of Forestry Research*, 28(1), 145–153.
- Kaskaoutis, D. G., Rashki, A., Houssos, E. E., Mofidi, A., Goto, D., Bartzokas, A., Francois, P., & Legrand, M. (2015). Meteorological aspects associated with dust storms in the Sistan region, southeastern Iran. *Climate Dynamics*, 45(1–2), 407–424.
- Kharazmi, R., Panidi, E. A., & Karkon, V. M. (2016). Assessment of dry land ecosystem dynamics based on time series of satellite images. *Sovremennyye problemy distantsionnogo zondirovaniya Zemli iz kosmosa*, 13(5), 214–223 (In Russian).
- Kharazmi, R., Abdollahi, A. A., Rahdari, M. R., & Karkon varnosfaderani, M. (2017a). Land cover monitoring and its impacts on land degradation and desertification trend using Landsat images (a case study of eastern Iran, Hamoun wetlands). *Arid Regions Geographic Studies*, 7(25), 64–75 (In Persian).
- Kharazmi, R., Panidi, E. A., & Chaban, L. N. (2017b). Assessment of arid ecosystems dynamics based on the results of automatized processing of multispectral satellite imagery time series. *Sovremennyye problemy distantsionnogo zondirovaniya Zemli iz kosmosa*, 14(3), 196–205 (In Russian).
- Kiage, L. M., Liu, K. B., Walker, N. D., Lam, N., & Huh, O. K. (2007). Recent land cover/use change associated with land degradation in the Lake Baringo catchment, Kenya, East Africa: evidence from Landsat TM and ETM+. *International Journal of Remote Sensing*, 28(19), 4285–4309.
- Kumar, P. J., Huan, T. L., Rossi, R. K., Yuan, Y., & Li, X. (2018). Color fusion of remote sensing images for imparting fluvial geomorphological features of river Yamuna and Ganga over Doon valley. *Journal of Geomatics*, 12(1), 270–286.
- Lasanta, T., Garcia-Ruiz, J. M., Perez-Rontome, C., & Sancho-Marcen, C. (2000). Runoff and sediment yield in a semi-arid environment: the effect of land management after farmland abandonment. *Catena*, 38(4), 265–278.
- Lasanta, T., Nadal-Romero, E., & Arnaez, J. (2015). Managing abandoned farmland to control the impact of re-vegetation on the environment. The state of the art in Europe. *Environmental Science & Policy*, 52, 99–109.
- Li, J., Kandakji, T., Lee, J. A., Tatarko, J., Blackwell III, J., Gill, T. E., & Collins, J. D. (2017). Blowing dust and highway safety in the southwestern United States: characteristics of dust emission “hotspots” and management implications. *Science of the Total Environment*, 621, 1023–1032.
- Lim, K., Treitz, P., Wulder, M., St-Onge, B., & Flood, M. (2003). LiDAR remote sensing of forest structure. *Progress in Physical Geography*, 27(1), 88–106.
- Lu, D., & Weng, Q. (2007). A survey of image classification methods and techniques for improving classification performance. *International Journal of Remote Sensing*, 28(5), 823–870.
- Luo, G. P., Zhou, C. H., Chen, X., & Li, Y. (2008). A methodology of characterizing status and trend of land changes in oases: a case study of Sangong River watershed, Xinjiang, China. *Journal of Environmental Management*, 88(4), 775–783.
- Luyssaert, S., Jammet, M., Stoy, P. C., Estel, S., Pongratz, J., Ceschia, E., Churkina, G., Don, A., Erb, K., Ferlicoq, M., Gielen, B., Grunwald, T., Houghton, R. A., Klumpp, K., Knohl, A., Kolb, T., Kuemmerle, T., Laurila, T., Lohila, A., Loustau, D., McGrath, M. J., Meyfroidt, P., Moors, E. J., Naudts, K., Novick, K., Otto, J., Pilegaard, K., Pio, C. A., Rambal, S., Rebmann, C., Ryder, J., Suyker, A. E., Varlagin, A., Wattenbach, M., & Dolman, A. J. (2014). Land management and land-cover change have impacts of similar magnitude on surface temperature. *Nature Climate Change*, 4(5), 389–393.
- Maleki, S., Soffianian, A. R., Soltani Koupaei, S., Saatchi, S., Pourmanafi, S., & Sheikholeslam, F. (2016). Habitat mapping as a tool for water birds conservation planning in an arid zone wetland: the case study Hamun wetland. *Ecological Engineering*, 95, 594–603.
- Maleki, S., Soffianian, A. R., Koupaei, S. S., Pourmanafi, S., & Saatchi, S. (2018). Wetland restoration prioritizing, a tool to reduce negative effects of drought; an application of multicriteria-spatial decision support system (MC-SDSS). *Ecological Engineering*, 112, 132–139.
- Maman, S., Orlovsky, L., Blumberg, D. G., Berliner, P., & Mamedov, B. (2011). A landcover change study of takyr surfaces in Turkmenistan. *Journal of Arid Environments*, 75(9), 842–850.
- Mandanici, E., & Bitelli, G. (2015). Multi-image and multi-sensor change detection for long-term monitoring of arid environments with Landsat series. *Remote Sensing*, 7, 14019–14038.
- Matinfar, H. R., Panah, S. K. A., Zand, F., & Khodaei, K. (2013). Detection of soil salinity changes and mapping land cover types based upon remotely sensed data. *Arabian Journal of Geosciences*, 6(3), 913–919.
- Mirzaei, M., Solgi, E., & Salmanmahiny, A. (2016). Assessment of impacts of land use changes on surface water using L-THIA model (case study: Zayandehrud river basin). *Environmental Monitoring and Assessment*, 188(12), 690.
- Mitsch, W. J., & Gosselink, J. G. (2000). The value of wetlands: importance of scale and landscape setting. *Ecological Economics*, 35(1), 25–33.
- Moosavi, V., Moradi, H., Shamsi, S. R. F., & Shirmohammadi, B. (2014). Assessment of the planimetric morphology of barchan dunes. *Catena*, 120, 12–19.
- Mousavi-Sabet, H., Gharaei, A., Nasrollahzade, A., Habibi, A., & Eagderi, S. (2014). Redescription of *Paracobitis rhadinaea* (Regan, 1906) from Sistan Basin, Iran (Teleostei: Nemacheiliidae). *International Journal of Aquatic Biology*, 2(5), 286–291.
- Munyati, C. (2000). Wetland change detection on the Kafue Flats, Zambia, by classification of a multitemporal remote sensing image dataset. *International Journal of Remote Sensing*, 21(9), 1787–1806.
- Najafi, A., & Vatanfada, J. (2011). Environmental challenges in trans-boundary waters, case study: Hamoon Hirmand wetland (Iran and Afghanistan). *International Journal of Water Resources and Arid Environments*, 1(1), 16–24.
- Najafinasab, F., Karbassi, A. R., & Ghoddousi, J. (2015). Fuzzy analytic network process approach to evaluate land and sea criteria for land use planning in coastal areas. *Ocean and Coastal Management*, 116, 368–381.
- Nazari Samani, A. A., Chen, Q., Khalighi, S., Wasson, R. J., & Rahdari, M. R. (2016a). Assessment of land use impact on

- hydraulic threshold conditions for gully head cut initiation. *Hydrology and Earth System Sciences*, 20(7), 3005–3012.
- Nazari Samani, A. A., Khosravi, H., Mesbahzadeh, T., Azarakhshi, M., & Rahdari, M. R. (2016b). Determination of sand dune characteristics through geomorphometry and wind data analysis in Central Iran (Kashan Erg). *Arabian Journal of Geosciences*, 9(18), 716–731.
- Nazari Samani, A. A., Wasson, R. J., Rahdari, M. R., & Moeini, A. (2016c). Quantifying eroding head cut detachment through flume experiments and hydraulic thresholds analysis. *Environmental Earth Sciences*, 75(21), 1424–1437.
- Nearing, M. A., Polyakov, V. O., Nichols, M. H., Hernandez, M., Li, L., Zhao, Y., & Armendariz, G. (2017). Slope–velocity equilibrium and evolution of surface roughness on a stony hillslope. *Hydrology and Earth System Sciences*, 21(6), 3221–3229.
- Okin, G. S., & Gu, J. (2015). The impact of atmospheric conditions and instrument noise on atmospheric correction and spectral mixture analysis of multispectral imagery. *Remote Sensing of Environment*, 164, 130–141.
- Othman, Y., Steele, C., & Hilaire, R. S. (2018). Surface reflectance climate data records (CDRs) is a reliable Landsat ETM+ source to study chlorophyll content in pecan orchards. *Journal of the Indian Society of Remote Sensing*, 46(2), 211–218.
- Padonou, E. A., Lykke, A. M., Bachmann, Y., Idohou, R., & Sinsin, B. (2017). Mapping changes in land use/land cover and prediction of future extension of bowé in Benin, West Africa. *Land Use Policy*, 69, 85–92.
- Patino, J. E., & Estupinan-Suarez, L. M. (2016). Hotspots of wetland area loss in Colombia. *Wetlands*, 36(5), 935–943.
- Pekel, J.-F., Cottam, A., Gorelick, N., & Belward, A. S. (2016). High-resolution mapping of global surface water and its long-term changes. *Nature*, 540(7633), 418–422.
- Pourghasemi, H. R., Pradhan, B., & Gokceoglu, C. (2012). Application of fuzzy logic and analytical hierarchy process (AHP) to landslide susceptibility mapping at Haraz watershed, Iran. *Natural Hazards*, 63(2), 965–996.
- Pulido-Fernández, M., Schnabel, S., Lavado-Contador, J. F., Mellado, I. M., & Pérez, R. O. (2013). Soil organic matter of Iberian open woodland rangelands as influenced by vegetation cover and land management. *Catena*, 109, 13–24.
- Qin, Y., Xiao, X., Wang, J., Dong, J., Ewing, K., Hoagland, B., Hough, D. J., Fagin, T. D., Zou, Z., Geissler, G. L., Xian, G. Z., & Loveland, T. R. (2016). Mapping annual forest cover in sub-humid and semi-arid regions through analysis of Landsat and PALSAR imagery. *Remote Sensing*, 8(11), 933.
- Rachael, F., Richard, T., Yi, L., & Simon, J. (2011). Landsat mapping of annual inundation (1979–2006) of the Macquarie marshes in semi-arid Australia. *International Journal of Remote Sensing*, 32(16), 4545–4569.
- Rahdari, G. R., Rahdari, M. R., Fakhireh, A., Shahryari, A. R., & Khosravi, H. (2013). GIS-based monitoring and EWSs of desertification (case study; southeastern of Iran). *International Journal of Advanced Biological and Biomedical Research*, 1(10), 1185–1198.
- Rahman, M. T. (2016). Detection of land use/land cover changes and urban sprawl in Al-Khobar, Saudi Arabia: an analysis of multi-temporal remote sensing data. *ISPRS International Journal of Geographical Information*, 5(2), 15.
- Ranjeet, J., Jiquan, C., Nan, L., & Burkhard, W. (2009). Land cover/land use change in semi-arid Inner Mongolia: 1992–2004. *Environmental Research Letters*, 4(4), 045010.
- Rashki, A., Kaskaoutis, D. G., Goudie, A. S., & Kahn, R. A. (2013). Dryness of ephemeral lakes and consequences for dust activity: the case of the Hamoun drainage basin, south-eastern Iran. *Science of the Total Environment*, 463, 552–564.
- Rashki, N., Rahdari, G. R., & Rahdari, M. R. (2014). Identification of detachment zone facieses (case study: Konarak region). *European Journal of Experimental Biology*, 4(3), 108–114.
- Rebelo, A. J., Scheunders, P., Esler, K. J., & Meire, P. (2017). Detecting, mapping and classifying wetland fragments at a landscape scale. *Remote Sensing Applications: Society and Environment*, 8, 212–223.
- Rezaei, R., & Ghofranfarid, M. (2018). Rural households' renewable energy usage intention in Iran: extending the unified theory of acceptance and use of technology. *Renewable Energy*, 122, 382–391.
- Rezaei Moghaddam, M. H., & Saghafi, M. (2006). A change detection application on the evolution of Kahak playa (South Khorasan province, Iran). *Environmental Geology*, 51(4), 565–579.
- Rezazadeh, M., Irannejad, P., & Shao, Y. (2013). Climatology of the Middle East dust events. *Aeolian Research*, 10, 103–109.
- Roy, D. P., Wulder, M. A., Loveland, T. R., Woodcock, C. E., Allen, R. G., Anderson, M. C., Helder, D., Irons, J. R., Johnson, D. M., Kennedy, R., et al. (2014). Landsat-8: science and product vision for terrestrial global change research. *Remote Sensing of Environment*, 145, 154–172.
- Ruan, R., Zhang, Y., & Zhou, Y. (2008). Change detection of wetland in Hongze Lake using a time series of remotely sensed imagery. *The International Archives of the Photogrammetry, Remote Sensing and Spatial Information Sciences*, 37, 1545–1548.
- Sabr, A., Moeinaddini, M., Azamivand, H., & Guinot, B. (2016). Assessment of land use and land cover change using spatio-temporal analysis of landscape: case study in south of Tehran. *Environmental Monitoring and Assessment*, 188(12), 691–705.
- Sakieh, Y., & Salmanmahiny, A. (2016). Performance assessment of geospatial simulation models of land-use change a landscape metric-based approach. *Environmental Monitoring and Assessment*, 188(3), 169.
- Santos, M. M., Machado, I. E. S., Carvalho, E. V., Viola, M. R., & Giongo, M. (2017). Estimation of forest parameters in Cerrado area from OLI Landsat 8 sensor. *Floresta*, 47(1), 75–83.
- Schmugge, T. J., Kustas, W. P., Ritchie, J. C., Jackson, T. J., & Rango, A. (2002). Remote sensing in hydrology. *Advances in Water Resources*, 25(8), 1367–1385.
- Schulz, J. J., Cayuela, L., Echeverria, C., Salas, J., & Rey Benayas, J. M. (2010). Monitoring land cover change of the dryland forest landscape of Central Chile (1975–2008). *Applied Geography*, 30(3), 436–447.
- Shafie, H., Amiri, I., Shahriari, A. R., Fakhireh, A., Noori, S., & Hosseini, S. M. (2011). RS-based assessment of vegetation cover changes in sistán plain. *African Journal of Social Sciences*, 1, 159–167.
- Shajaat Ali, A. M. (2006). Rice to shrimp: land use/land cover changes and soil degradation in southwestern Bangladesh. *Land Use Policy*, 23(4), 421–435.

- Sharifikia, M. (2013). Environmental challenges and drought hazard assessment of Hamoun Desert Lake in Sistan region, Iran, based on the time series of satellite imagery. *Natural Hazards*, 65(1), 201–217.
- Shengbo, C., & Rao, P. (2008). Land degradation monitoring using multi temporal Landsat TM/ETM data in a transition zone between grassland and cropland of Northeast China. *International Journal of Remote Sensing*, 29(7), 2055–2073.
- Siegal, B. S., & Gillespie, A. R. (1980). *Remote sensing in geology*, 702p. New York: Wiley.
- Silva, B., Alava-Nunez, P., Strobl, S., Beck, E., & Bendix, J. (2017). Area-wide evapotranspiration monitoring at the crown level of a tropical mountain rain forest. *Remote Sensing of Environment*, 194, 219–229.
- Sosnowski, A., Ghoneim, E., Burke, J. J., Hines, E., & Halls, J. (2016). Remote regions, remote data: a spatial investigation of precipitation, dynamic land covers, and conflict in the Sudd wetland of South Sudan. *Applied Geography*, 69, 51–64.
- Szczypta, C., Gascoïn, S., Houet, T., Hagolle, O., Dejoux, J. F., Vigneau, C., & Fanise, P. (2015). Impact of climate and land cover changes on snow cover in a small Pyrenean catchment. *Journal of Hydrology*, 521, 84–99.
- Tareq, S. M., Tanaka, N., & Ohta, K. (2004). Biomarker signature in tropical wetland: lignin phenol vegetation index (LPVI) and its implications for reconstructing the paleoenvironment. *Science of the Total Environment*, 324, 91–103.
- The Ramsar Convention on wetlands (2014). The list of wetlands of international importance. <http://archive.ramsar.org/pdf/sitelist.pdf>.
- Vahtmäe, E., & Kutser, T. (2013). Classifying the Baltic Sea shallow water habitats using image-based and spectral library methods. *Remote Sensing*, 5, 2451–2474.
- Vekerdy, Z., Dost, R., Reinink, G., & Partow, H. (2006). *History of environmental change in the Sistan Basin based on satellite image analysis: 1976–2005*. Geneva: UNEP.
- Verburg, P. H., Neumann, K., & Nol, L. (2011). Challenges in using land use and land cover data for global change studies. *Global Change Biology*, 17(2), 974–989.
- Verstappen, H.T. (1977). Remote sensing in geomorphology (No. 04; GB400. 42. R4, V4.). Elsevier Scientific Publishing Company.
- Vesali Naseh, M. R., Karbassi, A. R., Ghazaban, F., & Baghvand, A. (2012a). Evaluation of heavy metal pollution in Anzali wetland, Guilan, Iran. *Iranian Journal of Toxicology*, 5(15), 565–576.
- Vesali Naseh, M. R., Karbassi, A. R., Ghazaban, F., Baghvand, A., & Mohammadzadeh, M. J. (2012b). Magnetic susceptibility as a proxy to heavy metal content in the sediments of Anzali wetland, Iran. *Iranian Journal of Environmental Health Science & Engineering*, 9(1), 34–46.
- Vogelmann, J. E., Gallant, A. L., Shi, H., & Zhu, Z. (2016). Perspectives on monitoring gradual change across the continuity of Landsat sensors using time-series data. *Remote Sensing of Environment*, 185, 258–270.
- Whitney, J.W. (2006). Geology, water, and wind in the lower Helmand basin, southern Afghanistan U.S. Geological Survey, Reston, Virginia, Retrieved 2010-08-31.
- Wu, J. (2004). Effects of changing scale on landscape pattern analysis: scaling relations. *Landscape Ecology*, 19(2), 125–138.
- Wulder, M. A., Masek, J. G., Cohen, W. B., Loveland, T. R., & Woodcock, C. E. (2012). Opening the archive: how free data has enabled the science and monitoring promise of Landsat. *Remote Sensing of Environment*, 122, 2–10.
- Xiao, L., Wang, J., Dang, Y., Cheng, Z., Huang, T., Zhao, J., Xu, Y., Huang, J., Xiao, Z., & Komatsu, G. (2017). A new terrestrial analogue site for Mars research: the Qaidam Basin, Tibetan Plateau (NW China). *Earth-Science Reviews*, 164, 84–101.
- Yli-Pelkonen, V. (2008). Ecological information in the political decision making of urban land-use planning. *Journal of Environmental Planning and Management*, 51(3), 345–362.
- Yousefi, S., Keesstra, S., Pourghasemi, H. R., Surian, N., & Mirzaee, S. (2017). Interplay between river dynamics and international borders: the Hirmand River between Iran and Afghanistan. *Science of the Total Environment*, 586, 492–501.
- Yuan, Y., Li, B., Gao, X., Liu, H., Xu, L., & Zhou, C. (2016). A method of characterizing land-cover swap changes in the arid zone of China. *Frontiers of Earth Science*, 10(1), 74–86.
- Zehtabian, G.R., Mashhadi, N., Khosravi, H., Pour Reza, M., Rahdari, M.R., Kharazmi, R. (2014). Assessment of anthropogenic effect on land degradation. Proceeding: Anthropogenic changes of environment and landscape in arid and semi-arid regions (GIAN), University of Tehran, Tehran, pp 117–1129.
- Zewdie, W., & Csaplovics, E. (2015). Remote sensing based multi-temporal land cover classification and change detection in northwestern Ethiopia. *European Journal of Remote Sensing*, 48, 121–139.
- Zein, A. B., Mikheikin, S. V., Rogacheva, V. B., Zansokhova, M. F., Sybachin, A. V., & Yaroslavov, A. A. (2015). Polymeric stabilizers for protection of soil and ground against wind and water erosion. *Advances in Colloid and Interface Science*, 226, 17–23.
- Zolfaghari, G. H., Delsooz, M., & Rajaei, S. (2016). Study of mercury pollution in water, sediments, and fish from Hamoon international wetland. *Water and Wastewater*, 27(105), 25–37 (In Persian).